Data–driven Approach for Extracting Steady–state Data from Unsteady–state Flow Stress without Material Modeling

Eiichi Ota[1*], *Minami* Fujimura[1], and *Yasumoto* Sato[1]

[1]Toyota Central R&D Labs., Inc., 41–1 Yokomichi, Nagakute, Aichi 480–1192, Japan

Abstract. To accurately calculate the deformation behavior in forming simulations, it is essential to collect steady–state material properties and input them into the simulation software. For instance, in heated sheet metal forming processes, the temperature and strain rate change significantly. Hence, collecting data under isothermal and constant strain–rate conditions is crucial for representing such complex deformation behaviors. However, collecting steady–state data requires appropriate experimental apparatus or specimen geometry and precise control of the experimental environment. An alternative approach is the inverse analytical method, which identifies steady–state data by comparing forming simulation data with experimental measurements. However, this method requires material modeling that accurately represents the unsteady–state of a target. To overcome these challenges, we propose a simple method for directly extracting steady–state data by interpolating unsteady–state data using a machine learning method without material modeling. This paper describes a case study on the extraction of steady–state flow stress from high–temperature tensile experiments on a magnesium alloy sheet (AZ31) using Gaussian process regression. The results demonstrated that the flow stress extracted using the proposed method has predictive accuracy equivalent to that obtained through inverse analysis with a predefined material model that can express the dependency on the temperature and strain rate.

Keywords: Machine learning; material properties; unsteady state; material modeling.

1 Introduction

Shortening the product development period is important to flexibly and quickly develop products in response to changes in societal demand. Numerical calculation methods such as forming simulations are effective in shortening the development period because they enable the consideration of countermeasures for potential problems in the early phases of development [1]. In recent years, there have been reports on the use of regression models called surrogate models that are trained on the results of hundreds to thousands of forming simulations, to more quickly determine appropriate manufacturing conditions compared to standard forming simulations [2]. High–precision forming simulations are essential for shortening the development period.

To accurately calculate the deformation behavior in a forming simulation, it is necessary to collect the steady–state material properties and input them into the simulation software. For example, in heated sheet metal forming processes, such as hot stamping [3], temperature and strain rate significantly change during the forming process. Hence, collecting data under isothermal and constant strain–rate conditions corresponding to each moment of the unsteady state is important for expressing such complex deformation behaviors. During the forming process, the high–temperature material comes into contact with cold dies, leading to a partial temperature decrease and strength distribution within the material [4]. In addition, it is important to consider the effect of the strain rate on the formability to conduct high–precision forming simulations [5].

However, when collecting steady–state data for forming simulations, it is difficult to devise an appropriate experimental apparatus and specimen shape to conduct steady–state experiments [6] and precisely control the tensile speed, temperature, and atmosphere [7]. In another approach, an inverse analytical method is used to identify the parameters of the material model or steady–state material properties set in the forming simulation by comparing the forming simulation data with the experimental measurement data [8]. However, this approach requires a material modeling that can accurately express the unsteady state of the target [9]. In the study by Li et al. [10], a neural network–augmented mixed Swift–Voce strain hardening law was employed as a material model to capture the temperature– and strain–rate–dependence of aluminum alloy sheets. The implementation of this approach requires advanced expertise in material modeling and iterative simulations for inverse analysis.

To address these difficulties, we propose a simple method that enables us to directly extract steady–state data by interpolating unsteady–state data using machine learning methods without material modeling.

* Corresponding author: e–ota@mosk.tytlabs.co.jp

Specifically, as shown in Fig. 1, if unsteady–state data can be interpolated using regression analysis in machine learning, it would be possible to directly extract steady–state data without designating a material model. This paper describes a case study for extracting steady–state flow stress (true stress and logarithmic plastic strain relationship) from measurement data in high–temperature tensile experiments of a magnesium alloy sheet (AZ31) using a statistical inference method called Gaussian process regression (GPR) [11]. To discuss the usability of the proposed method, it was compared with a regression model—the temperature– and strain–rate–dependent power–law hardening model (hereinafter referred to as the reference regression model) reported by Tari et al. [12].

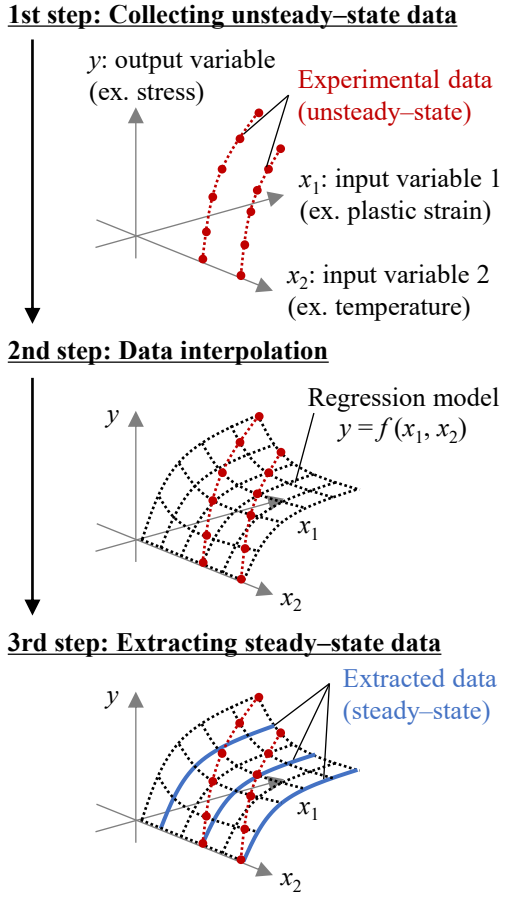

Fig. 1. Procedure for extracting steady–state data by interpolating unsteady–state data using the regression model.

2 Methods

Assuming that the true stress is determined by the logarithmic plastic strain, temperature, and strain rate, the flow stress under isothermal and constant strain–rate conditions was extracted via the following three steps.

- 1st step: Collecting unsteady–state data (Section 2.1)
- 2nd step: Data interpolation (Section 2.2)
- 3rd step: Extracting steady–state data (Section 2.3)

2.1 Collecting unsteady–state data

High–temperature tensile experiments were conducted on heated specimens in a room–temperature environment without atmospheric or constant–temperature control. A 1.0 mm thick magnesium alloy sheet (AZ31) was used as the specimen. As reported in [12], the flow stress of a magnesium alloy sheet depends on the temperature and strain rate. To accurately evaluate the formability at elevated temperatures in forming simulations, it is necessary to collect flow stress data that depend on the temperature and strain rate. Therefore, in this study, experiments were conducted in a warm forming temperature range (25–300°C), assuming actual press forming speed ranges (strain rate: 0.25–0.025 s^{-1}).

The dimensions of the specimens are shown in Fig. 2. A specimen with a parallel section width of 8 mm and length of 22 mm was used. The configuration of the experimental apparatus is shown in Fig. 3. A thermomechanical processing simulator (Thermec–mastor–Z, Fuji Electronic Industrial Co., Ltd.) was used as the tensile experimental apparatus. The specimen was heated via Joule heating. The heating rate was set to 20 °C/s. The heating rate was controlled by proportional–integral–differential (PID) control using an R–type thermocouple welded to the center of the specimen.

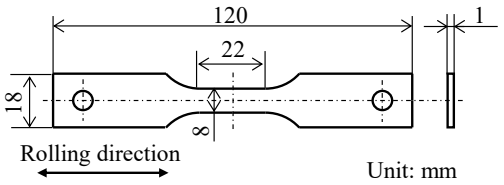

Fig. 2. Specimen dimensions.

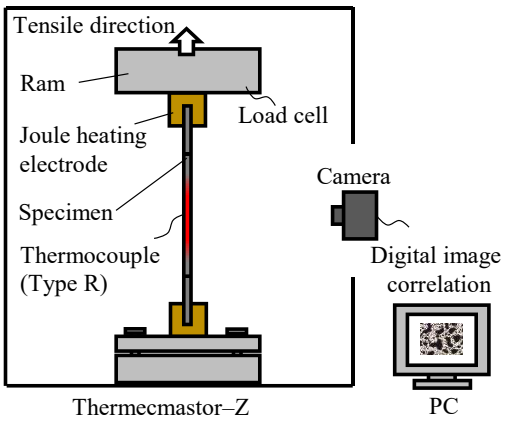

Fig. 3. Schematic diagram of the tensile experimental setup.

The experimental conditions are listed in Table 1. A total of 12 experiments were performed under different temperature and strain conditions (Nos. 1–12). Nos. 1, 5, and 9 were conducted at room temperature (25°C) without heating the specimens. For other experimental data, high–temperature tensile experiments were conducted during air cooling after heating to 400°C. The tensile experiment was started when the temperature dropped to around 300, 200, and 100°C, based on the cooling history shown in Fig. 4. The ram speed was set to 5.5–0.55 mm/s, so that the apparent strain rate (ram speed/parallel section length) matched the actual press forming speed range (0.25–0.025 s^{-1}). Based on the cooling history in Fig. 4, the estimated temperature drop to a nominal strain of 0.1 for experiment No. 4 (approximate initial tensile temperature: 300°C and

apparent strain rate: 0.25 s^{-1}) is approximately 10°C over a tensile duration of 0.4 s. In contrast, for experiment No. 12 (approximate initial tensile temperature: 300°C and apparent strain rate: 0.025 s^{-1}), the temperature drop is approximately 70°C over a tensile duration of 4 s.

The in–plane displacement distribution during the tensile experiment was measured using the digital image correlation (DIC) method, based on the transformation behavior of a black random pattern. This random pattern was applied by spraying the specimen with a black spray from a certain distance. Strain analysis of the in–plane displacement distribution was conducted using the image correlation analysis software VIC–2D (Correlated Solutions, Inc.). The deformation behavior was recorded using a digital camera that captured full HD videos at a frame rate of 59.94 fps. Additionally, the field of view in the longitudinal direction (tensile direction) was set to 85–90 mm, so that each pixel represented 50 µm.

Table 1. Experimental conditions.

Apparent strain rate [s^{-1}] (Ram speed [mm/s])	Approximate tensile starting temperature [°C]			
	25	100	200	300
0.25 (5.5)	No. 1	No.2	No. 3	No. 4
0.1 (2.2)	No. 5	No. 6	No. 7	No. 8
0.025 (0.55)	No. 9	No. 10	No. 11	No. 12

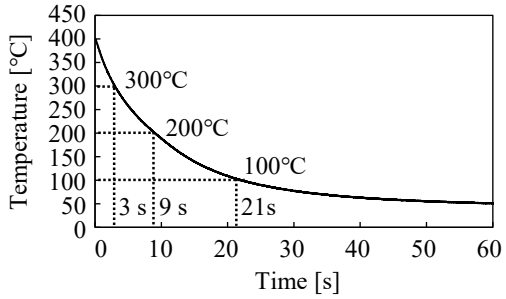

Fig. 4. Cooling history.

Fig. 5 shows an example of a camera image captured during the deformation of experiment No. 4 and an image in which the nominal strain distribution is mapped by DIC. In this experiment, the specimen was heated via Joule heating; thus, the areas other than the parallel section were barely heated. Therefore, the temperature was distributed along the longitudinal direction during the experiment, which led to strain distribution along the same direction. In other words, when calculating the true stress precisely, a uniform deformation should not be assumed across the entire parallel section. In this experiment, to calculate the true stress, deformation in the tensile and width directions at the position with the largest deformation in the longitudinal direction was determined using an image correlation method. The logarithmic plastic strain range of 0–0.1, where data exist for all experiments, was targeted to examine the interpolation method of the experimental data in this study. The logarithmic plastic strain was obtained by subtracting the elastic strain from the measured data, using the temperature–dependent Young's modulus of the magnesium alloy sheet as described in reference [13].

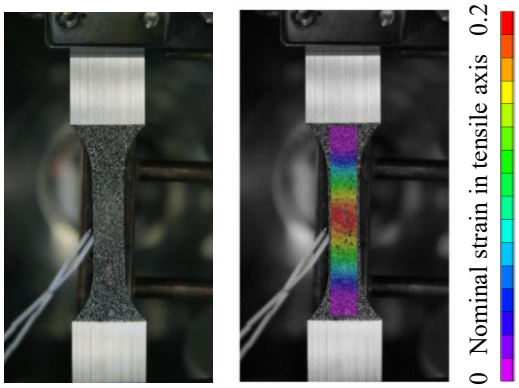

(a) Camera image (b) DIC processed image

Fig. 5. Strain map analyzed by DIC. (No. 4: approximate tensile starting temperature, 300°C; apparent strain rate, 0.25 s^{-1})

Fig. 6 shows the flow stress data obtained from each experiment. The interpolation method based on the unsteady–state data is described in the following section. Fig. 7 shows the results of No. 11 (approximate initial tensile temperature: 200°C and apparent strain rate: 0.025 s^{-1}) as an example of the changes in temperature and strain rate during the tensile experiment. During the tensile experiment, the temperature decreased from 186.6 to 131.2°C, and the strain rate increased from 0.006 to 0.022 s^{-1}.

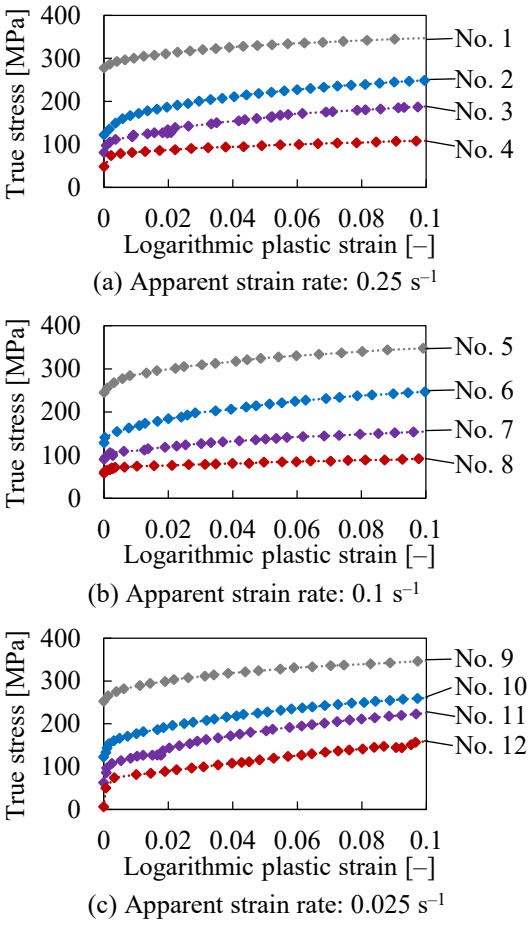

(a) Apparent strain rate: 0.25 s^{-1}

(b) Apparent strain rate: 0.1 s^{-1}

(c) Apparent strain rate: 0.025 s^{-1}

Fig. 6. Flow stress data collected by tensile experiment.

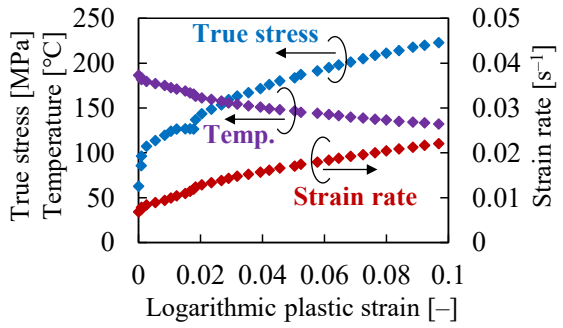

Fig. 7. Temperature and strain rate changes during tensile experiments (No. 11: approximate tensile starting temperature, 200°C; apparent strain rate, 0.025 s^{-1}).

2.2 Data interpolation

The collected unsteady–state data were interpolated by applying the GPR [11], which is a machine learning method, without material modeling. The GPR model was implemented in Python using the GPy library. The experimental data of Nos. 6 and 7 were used as test data, and the remaining ten data were used as training data. The test data were selected within the range of the training data. The root mean square error (RMSE) shown in Eq. (1) was used as the evaluation index for prediction accuracy.

$$\mathrm{RMSE} = \sqrt{\frac{1}{n}\sum_{i=1}^{n}(y_i - \hat{y}_i)^2}, \tag{1}$$

where y_i is the i–th test data out of n data points, and $\hat{y}_i$ is the i–th predicted data point.

The GPR is a regression model that uses the probability distribution of a random function called the Gaussian process. One advantage of GPR is that it does not require the specification of a functional form for the regression model. This flexibility allows GPR to adapt to various types of data without a predefined material model. The GPR predicts the output values for new inputs by assuming that the outputs follow a normal distribution. It uses the relationships between known data points to make predictions, providing both the predicted mean and variance. In other words, given the training data $(x_1, y_1), (x_2, y_2), \cdots, (x_n, y_n)$, the mean $\mu(x_{new})$ and variance $\sigma^2(x_{new})$ of the output value (y_{new}) to be predicted for a new input (x_{new}) can be expressed by Eqs. (2) and (3), respectively.

$$\mu(x_{new}) = \boldsymbol{k}_{new}^T \boldsymbol{K}^{-1} \boldsymbol{y} \tag{2}$$

$$\sigma^2(x_{new}) = k(x_{new}, x_{new}) - \boldsymbol{k}_{new}^T \boldsymbol{K}^{-1} \boldsymbol{k}_{new} \tag{3}$$

Here, $\boldsymbol{K}$ is the covariance matrix consisting of kernels $k(x_i, x_j)$, which represents the relationship between the two input values x_i and x_j. The ii component is ${\sigma_i}^2$, and the ij component is $k(x_i, x_j)$. $\boldsymbol{k_{new}}$ is a vector formed by arranging the kernel values between the new input x_{new} and training data inputs $\boldsymbol{x}$, which can be represented as $[k(x_{new}, x_1), k(x_{new}, x_2), \cdots, k(x_{new}, x_n)]^T$.

Kernel k expresses the similarity between two data points, and the three commonly used types of kernels are shown in Eqs. (4), (5), and (6).

・RBF kernel

$$k(\boldsymbol{x}, \boldsymbol{x}') = \theta_1 * \exp\left(-\frac{\|\boldsymbol{x} - \boldsymbol{x}'\|^2}{2{\theta_2}^2}\right) \tag{4}$$

・Matern 5/2 kernel

$$k(\boldsymbol{x}, \boldsymbol{x}') = \theta_1 * \left(1 + \frac{\sqrt{5}\|\boldsymbol{x} - \boldsymbol{x}'\|}{\theta_2} + \frac{5\|\boldsymbol{x} - \boldsymbol{x}'\|^2}{3{\theta_2}^2}\right) * \exp\left(-\frac{\sqrt{5}\|\boldsymbol{x} - \boldsymbol{x}'\|}{\theta_2}\right) \tag{5}$$

・Matern 3/2 kernel

$$k(\boldsymbol{x}, \boldsymbol{x}') = \theta_1 * \left(1 + \frac{\sqrt{3}\|\boldsymbol{x} - \boldsymbol{x}'\|}{\theta_2}\right) * \exp\left(-\frac{\sqrt{3}\|\boldsymbol{x} - \boldsymbol{x}'\|}{\theta_2}\right) \tag{6}$$

Here, θ_1 and θ_2 are hyperparameters. These can be determined using the maximum likelihood estimation method provided by the GPy library in Python, without requiring any manual adjustments.

In this study, the GPR models were trained using each of the three kernel types, and the model with the smallest prediction error for the test data was selected. As the numerical scales of the input variables differed, the data were normalized to values between 0 and 1 for each variable. Additionally, an automatic relevance determination (ARD) feature was used to optimize the hyperparameters of kernel k for each input variable.

To discuss the usability of the method extracted using the proposed approach, the parameters of the reference regression model in Eq. (7) [12] were determined using the training data, and the prediction error for the test data was compared with that of the selected GPR model.

$$\sigma_{stress} = F(T) * (\varepsilon_0 + \varepsilon_p)^{n(T)} * \dot{\varepsilon}^{m(T)} \tag{7}$$

Here, σ_{stress} is the true stress [MPa], and ε_p is the logarithmic plastic strain. ε_0 is a material constant, and it was set to 0.002. The reference regression model is a power–law–based material model that depends on the temperature and strain rate. Furthermore, F, n, and m are functions of temperature T [K], as shown in Eqs. (8), (9), and (10), respectively.

$$F(T) = A_0 + A_1 * \left(1 - \exp(A_2 * (T - T_r)/T_m)\right) \tag{8}$$

$$n(T) = A_3 + A_4 * \left(1 - \exp(A_5 * (T - T_r)/T_m)\right) \tag{9}$$

$$m(T) = A_6 * \left(1 - \exp(A_7 * (T - T_r)/T_m)\right) \tag{10}$$

Here, T_r and T_m are the room temperature and melting temperature of Mg, respectively, which were set to 298 K (25°C) and 923 K (650°C), respectively. In this study, for each measured data point, the error was defined as the difference between the "true stress calculated using Eq. (7) from the measured logarithmic plastic strain, temperature, and strain rate" and the "true stress obtained experimentally." The coefficients A_0–A_7 were determined by minimizing the sum of these errors.

2.3 Extracting steady–state data

All the trained regression models in the previous section take the values of logarithmic plastic strain, temperature, and strain rate as inputs, and output the true stress value. These regression models can predict the true stress values within the design space (logarithmic plastic strain range: 0–0.1, temperature: 25–300°C, and strain rate:

0.025–0.25 s^{-1}). In this study, several flow stresses under constant temperature and strain–rate conditions were extracted as examples.

3 Results and discussion

Table 2 lists the parameters of the reference regression model described in Section 2.2. Fig. 8 shows the prediction results of the test data obtained using this reference regression model. The prediction error (RMSE) of the test data was 9.513 MPa. Considering that the maximum true stress within the design space of the test data was approximately 250 MPa, the prediction error was estimated to be approximately 4%.

Table 2. Reference regression model parameters.

A_0	A_1	A_2	A_3
430	−9191	−0.098	0.092

A_4	A_5	A_6	A_7
0.054	−10.616	12.074	−0.025

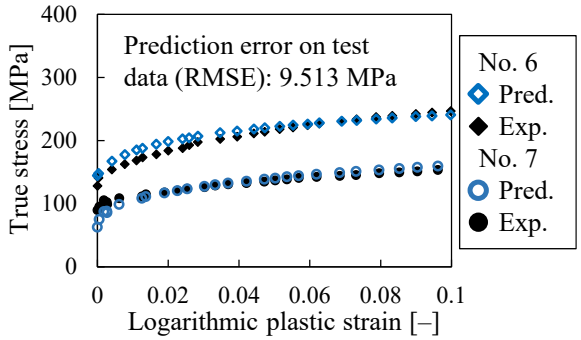

Fig. 8. Prediction results for the test data, obtained using the reference regression model.

To select an appropriate kernel function, the prediction errors of the test data obtained using the GPR models trained with the three different kernel functions were compared. Table 3 lists the prediction errors of the test data and fitting errors of the training data for the GPR models. The prediction error (RMSE) for the test data was 9.189 MPa when the Matern 5/2 kernel was used, which was the smallest among the three compared kernel functions. The Matern 3/2 kernel resulted in a larger prediction error for the test data than the other two kernels. However, the fitting error for the training data was small, which may indicate overfitting. Fig. 9 shows the results of the test data prediction obtained using the GPR model with the Matern 5/2 kernel, which exhibited the highest prediction accuracy. This prediction error was comparable to that of the reference regression model. Notably, the predicted results of No. 6 in Fig. 9 show better agreement with variations in true stress around a logarithmic plastic strain of 0.02 compared to the predictions in Fig. 8. These results suggest that the proposed method has the potential to train a regression model with a high prediction accuracy without a predefined material model. For reference, Fig. 10 displays the prediction results of the GPR model with the Matern 3/2 kernel, which exhibited the lowest prediction accuracy but the smallest fitting error, as noted in Table 3. The results obtained using this kernel indicate that it overfits the training data. Thus, an appropriate kernel type must be selected according to the test data. However, by setting the test data as in this study, the kernel with the smallest prediction error for the test data can be selected.

Table 3. Prediction error on test data and fitting error on training data in GPR for each kernel.

Kernel types for Gaussian process regression	Prediction error on test data [MPa]	Fitting error on training data [MPa]
RBF	9.221	3.308
Matern 5/2	9.189	3.254
Matern 3/2	25.975	0.944

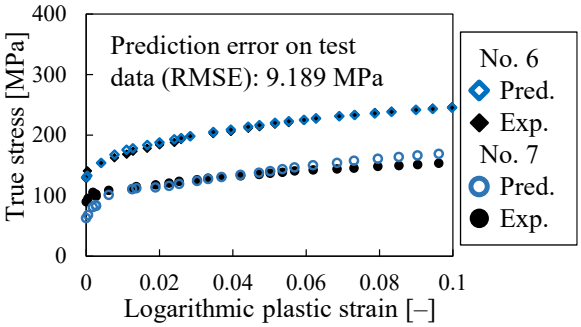

Fig. 9. Prediction results for test data using the GPR model with the Matern 5/2 kernel.

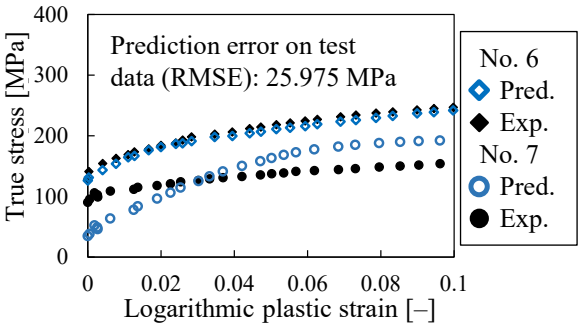

Fig. 10. Prediction results for test data using the GPR model with the Matern 3/2 kernel.

The results of extracting the steady–state flow stress using the GPR model with the Matern 5/2 kernel are shown in Fig. 11. Fig. 11(a) shows the isothermal flow stress at a constant strain rate of 0.1 s^{-1} (25, 100, 200, and 300°C), and Fig. 11(b) shows the extracted flow stress at constant strain rates (0.025, 0.1, and 0.25 s^{-1}) at isothermal conditions of 100 and 200°C. The results show that the higher the temperature, the lower the true stress, and the higher the strain rate, the lower the true stress, which is consistent with the findings of previous studies [12].

Fig. 12 shows the measured unsteady–state data of No. 11 and extracted steady–state data (isothermal flow stress at 100–200°C at a constant strain rate of 0.025 s^{-1}). The unsteady–state flow stress exhibited a steeper slope of true stress increase with increasing logarithmic

plastic strain compared to the extracted isothermal and constant–strain–rate flow stresses. This result suggests that this method can extract the flow stress, while excluding the effects of temperature decrease and strain–rate increase.

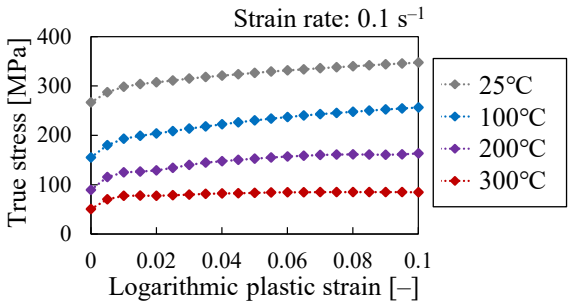

(a) Effects of temperature on flow stress at strain rate 0.1 s^{-1}

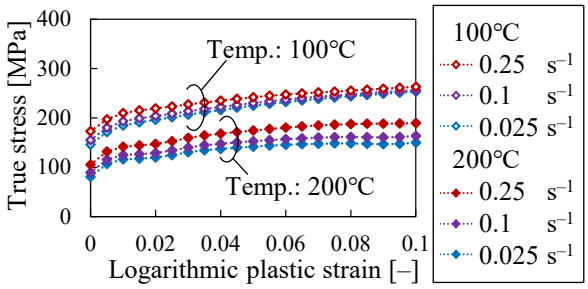

(b) Effects of strain rate on flow stress at 100°C and 200°C

Fig. 11. Examples of the extracted steady–state flow stress.

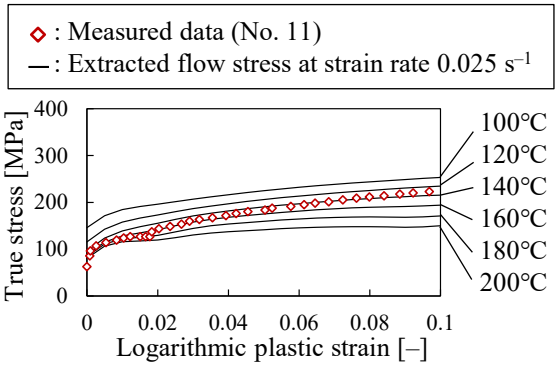

Fig. 12. Comparison of measured unsteady–state data with extracted steady–state data.

4 Conclusions

We propose a simple method that enables the direct extraction of the steady–state flow stress necessary for high–precision forming simulations by interpolating the unsteady–state data using a machine learning method without material modeling. This paper describes a case study for extracting steady–state flow stress from measured unsteady–state data in high–temperature tensile experiments of a magnesium alloy sheet (AZ31) using a statistical inference method called GPR, a machine learning method. The proposed method demonstrates the potential to extract steady–state data directly from unsteady–state data without using a predefined material model.

References

1. A. E. Tekkaya, J. Mater. Process. Technol. **103**, 14 (2000)
2. H. R. Attar, N. Li, IOP Conf. Ser. Mater. Sci. Eng. **1238**, 012066 (2022)
3. H. Karbasian, A. E. Tekkaya, J. Mater. Process. Technol. **210**, 2103 (2010)
4. E. Ota, Y. Yogo, N. Iwata, H. Nishigaki, J. Mater. Process. Technol. **263**, 198 (2019)
5. C. Zhang, L. Leotoing, D. Guines, E. Ragneau, J. Mater. Process. Technol. **209**, 3849 (2009)
6. R. Du, C. Mareau, Y. Ayed, E. Giraud, P. Dal Santo, J. Mater. Process. Technol. **281**, 116609 (2020)
7. H. W, Park, K. Kim, H. W. Park, J. Yanagimoto, ISIJ Int. **60**, 573 (2020)
8. A. Andrade–Campos, S. Coppieters, M. Strano, Int. J. Mater. Form. **15**, 44 (2022)
9. S. Sueki, A. Ishii, S. Coppieters, A. Yamanaka, Int. J. Solids Struct. **279**, 112350 (2023)
10. X. Li, C. C. Roth, K. Pandya, N. Karathanasopoulos, D. Mohr, IOP Conf. Ser. Mater. Sci. Eng. **1238**, 012006 (2022)
11. C. E. Rasmussen, C. K. I. Williams, MIT Press, (2006)
12. D. Ghaffari Tari, M. J. Worswick, J. Mater. Process. Technol. **221**, 40 (2015)
13. J. H. Kim, D. Kim, Y. S. Lee, M. G. Lee, K. Chung, H. Y. Kim, R. H. Wagoner, Int. J. Plast. **50**, 66 (2013)